Theoretical and Experimental Fluid/Structure Investigation of an On Demand Induced Spray

M. Tembely[a*], C. Lécot[b] and A. Soucemarianadin[a]
[a]Laboratory of Geophysical and Industrial Fluid Flows, UMR 5519, University Joseph Fourier, Grenoble, BP 53, 38041 Grenoble Cedex, France
[b]Laboratory of Applied Mathematics, UMR 5127 CNRS, University of Savoie, 73376 Le Bourget-du-Lac Cedex, France

Abstract

We report in this paper a physically based drop size distribution of a spray. The atomization is performed by a new Spray On Demand (SOD) device which exploits ultrasonic generation via a Faraday instability. The Modified Hamilton's principle is used to describe the fluid structure/interaction with a vibrating micro-channel conveying fluid excited by a pointwise piezoactuator, a non-equilibrium thermodynamics results is used allowing determining the volume flow rate generated by the tube motion. We combine to the fluid/structure description a physically based approach for predicting the drop-size distribution within the framework of the Maximum Entropy Formalism (MEF) using conservation laws of energy and mass coupling with the three-parameter generalized Gamma distribution. The prediction and experimental validation of the drop size distribution of a new Spray On Demand print-head is performed. Deriving an analytical expression estimating Sauter Mean Diameter (D_{32}) and Volume Mean Diameter (D_{30}), a validation of this model is also performed by comparing predictions with experimental results of drop size distribution. The dynamic model is shown to be sensitive to operating conditions, design parameters and physico-chemical properties of the fluid and its prediction capability is good. The approach avoids the traditional adjustment for each operating condition and has better predictive capabilities. We also report on a model allowing the study of the evolution of drop size-distribution. This model couples physically based Maximum Entropy Formalism and the Monte Carlo method to solve the temporal drop-size distribution equation in a continuous manner.

Introduction

Any manufacturing operation that requires the precise metering of materials to specified locations on substrates can take advantage of jet printing. It is well known that piezoelectric jet printing technology is capable of depositing controlled amounts of fluid onto a specified location very accurately. Combining this ability with an increasingly wide selection of fluids has made piezoelectric on-demand jetting system a promising device for developing innovative industrial applications. Jet printing technology offers an amazingly broad range of utilization in a wide range areas of applications such as biotechnology, electronics, pharmacology, micro-optics, and many others only limited by our imagination [1]. Four major fluid jetting techniques are well known: Drop On Demand (DOD), Continuous Ink Jet (CIJ), Electro-Valve and Spray Technologies. Our work will focus on an innovative spray technology, which may be qualified as a Spray On Demand (SOD) technology, where spray is generated only if required. This constitutes a major difference with classical spraying technologies where jetting is continuous.

Fluid (ink) jet print-heads offer the advantage of non-contact thus minimizing contamination. Generally classical print-heads are well adapted to applications dealing with Newtonian fluids. However a growing number of engineering applications need robust devices allowing ejection of rheologically complex fluids (like polymer, fluids with particles). In this paper, we give the underlying theory experimental validation for an innovative Spray On Demand printhead (SOD) [2].

Some of the numerous applications covered by this device concern the ejection of complex fluids for fuel cell fabrication or metallization (copper and gold electrodes) by electroless plating. The latter application is based on our pending patent and may be used on both impervious and porous substrates.

Spray Generation

A micro-channel conveying fluid (Fig. 1) is excited in an ultrasonic mode by a piezo-ceramic actuator (PZA), then the hung drop or film at the beveled nozzle tip break up into droplets via a Faraday instability. It is a parame-

*Corresponding author

tric resonance in which instability modes on hung drop at the SOD nozzle tip appear when a critical acceleration value is reached. The limit acceleration a_l in which droplet is generated depends on the exciting frequency f, fluid and nozzle (structure) properties. So when the limit acceleration at which film instability occur is known we easily can deduce the maximum amplitude of the film at which instability generates droplets leading to atomization.

$$A \propto a_l / f^2 \tag{1}$$

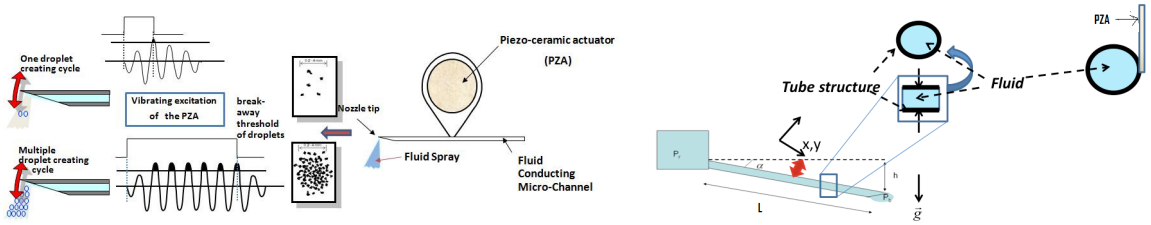

Figure 1. (a) Principle of Spray On Demand print-head operation (b) Problem statement

Piezoelectric Actuator Force Modeling

To compute the deformed shape of the tube, we need to compute the external force exerted on the tube; the force exerted has to generate spray formation at the tip of the tube. The SOD nozzle vibrates due to the soldered piezoelectric movement [3]. Here we propose to determine the force exerted by the PZA (of radius r_p) on the nozzle knowing the voltage wave form applied to the piezo-actuator; the force exerted by the PZA (of piezoelectric voltage constant g_{31}) at the nozzle with a varied exciting sine voltage (of amplitude A_p) is then:

$$F_p(t) = \frac{2\pi r_p A_p \sin(2\pi f t)}{g_{31}} \tag{2}$$

This temporal force and of sine form is not a restriction as any other force could be broken down through Fourier decomposition series. In addition, linking the force with the characteristics of PZA is a very useful approach for a comprehensive modeling of SOD. So that parametric studies and effect of PZA properties on SOD operation be possible.

Vibrating Micro-Channel Conducting Fluid General Equation of Motion

We consider the system as an approximation of the SOD shown in Fig. 1b. A straight cantilever tube is fixed along the x-axis. The fluid enters the tube at the fixed end and exits at the free end. At the middle of the tube is soldered a piezoelectric actuator (PZA) allowing transversal motion of the nozzle. The free end of the tube is beveled. Standard hypothesis for these development assumes, (i) the tube is of uniform annular cross-section, (ii) tube is long compared to its diameter (iii) effect of rotary inertia and shear deformation are ignored, (iv) center line of the tube is inextensible (v) tube is elastic and initially straight, (vi) plane sections remain plane and perpendicular to the beam axis (Bernoulli-Euler beam theory) (vii) effect of internal dissipation and damping are neglected.

It is to be stressed here that our analysis is not for high speed fluid where flutter instability (via a Hopf bifurcation) is observed once the flow velocity exceeds a critical velocity [4]. The dynamical stability analysis and flutter instability control of pipes conveying fluid has been done by many authors [5, 6]. For our case, let us establish the equation of motion using the elegant Hamilton's Principle taking into account nonlinear effects, print-head configurations, operating conditions, physical and mechanical properties of fluid and structure.

Hamilton formulation seems to be the most convenient for the study it could be formulated as follows [8]:

$$\delta \int_{t_1}^{t_2} \ell dt + \int_{t_1}^{t_2} \delta W dt = \int_{t_1}^{t_2} M_f U \left. \frac{d\vec{r}}{dt} \right|_L \delta \vec{r}_L dt \tag{3}$$

where M_f, U respectively are mass per unit length of the fluid and mean fluid velocity in the channel, δ being Hamilton operator.

We set $\vec{r} = (s+u(s,t))\vec{i} + v(s,t)\vec{j} = x\vec{i} + y\vec{j}$ the location of a material point on the tube, with s the curvilinear coordinate along the tube.

Kinetic energy of the system

The kinetic energy of the system consists of the kinetic energy of the fluid and of the tube:

$$K = K_f + K_t = \frac{1}{2}M_f \int_0^L (\frac{d\vec{r}}{dt})^2 ds + \frac{1}{2}m_t \int_0^L v_t{}^2 ds \tag{4}$$

Potential energy of the system

There are 2 components for the potential energy of the system. The strain energy of the tube V_{st} and gravitational energy V_g for both fluid and tube structure.

$$V = V_g + V_{st} = (m_t + M_f)g\left\{\cos\alpha \int_0^L y ds - \sin\alpha \int_0^L x ds\right\} + \frac{1}{2}EI\int_{t_1}^{t_2}\int_0^L \delta(\kappa^2) ds dt \tag{5}$$

Where the square curvature is given by $\kappa^2 = (\frac{\partial^2 u}{\partial s^2})^2 + (\frac{\partial^2 v}{\partial s^2})^2$ and α tube tilt angle.

Virtual work

The virtual work due to PZA displacement along the *y*-axis taking into account PZA force and moment is,

$$\int_{t_1}^{t_2}\delta W_F dt + \int_{t_1}^{t_2}\delta W_M dt = \int_{t_1}^{t_2}\int_0^L F(x,t)\delta y ds dt - \int_{t_1}^{t_2}\int_0^L F(x,t)\varsigma y''\delta y ds dt \tag{6}$$

With $F(x,t) = F_p(t)\delta(x - x_p)$, here δ is Dirac functional and x_p PZA position on the tube.

Applying Hamilton δ Operator, after some algebraic manipulations, one finally obtains the general non-linear equation of motion of the transversal displacement $v(x,t)$ due to PZA pointwise force:

$$\begin{aligned} &EI\left\{(1+v'^2)v'''' + (v''^3 + 4v'v''v''')\right\} + F(x,t)(\varsigma v'' - 1) + (m_t + M_f)\left\{\ddot{v} + v'\int_0^s (\dot{v}'^2 + v'\ddot{v}')ds - v''\int_0^s\int_s^L (\dot{v}'v' + v'\ddot{v}')ds ds\right\} \\ &+ (m_t + M_f)g\left\{\sin\alpha(v' + \frac{1}{2}v'^3) - \sin\alpha(L-s)(v'' + \frac{3}{2}v'^2 v'') + \cos\alpha\right\} + 2M_f U\left\{\dot{v}'(1+v'^2) - v''\int_s^L v'\dot{v}' ds\right\} + M_f U^2\left\{v''(1+v'^2) - v''\int_s^L v'v'' ds\right\} = 0 \end{aligned} \tag{7}$$

where prime (') and dot (.) respectively denotes for derivative with respect to *s* (or *x*) and time *t*. Equation (7) is then solved using Galerkin's method, as first approximation we neglect fluid and non-linear effect.

Vibrating Tube Flow Rate Estimation

Following irreversible (non-equilibrium) thermodynamics [7] expressing the proportionality near equilibrium between flux and force, in case of fluid flowing in the channel, we show that the flux (Q) could be expressed as [8]:

$$Q(t) = \rho k_p \frac{\pi\varsigma^4}{8\mu}\sqrt{\int_0^1 [(g - \ddot{v}(x,t))v'(x,t)]^2 dx} \tag{8}$$

k_p constant determined using experimental results.

Prediction of Spray On Demand Drop-Size Distribution

It is very important for spray applications to know the droplet size distribution of the nozzle used. One of the means to describe quantitatively a spray is thus to adopt the tools of statistical analysis. Following [9], there are three methods for modeling drop size distribution: Empirical Method, Probability Function Method and the Maximum Entropy formalism (MEF) which is the one adopted by us.

Mass Conservation

Let M_s be the equivalent mass of fluid ejected by the nozzle during a fixed excitation time T_p. We can express M_s differently in the following way:

$$M_s = \rho V_{ol} = \sum m_i = \sum \rho V_i \tag{9}$$

Where probability p_i is defined as $p_i = N_i / N$. From (9) we deduce the constraint upon mass conservation as

$$\sum_{i=1}^{N} p_i d_i^3 = 1 \quad \text{with } d_i = D_i / D_{30} \tag{10}$$

For hung drop at the tip of the micro-channel, by applying Newton second law, with a balance between inertial force, surface tension and gravity we deduce:

$$M_s(\bar{\gamma} + g) = \sigma C \cos\theta_E \tag{11}$$

A good approximation due to Ramanujan for the elliptical nozzle tip circumference is $C \approx \pi[3(a+b) - \sqrt{(3a+b)(a+3b)}]$

The acceleration and mean acceleration respectively of the nozzle tip could be deduced using (7) as,

$$\gamma(t) = \frac{\partial^2 v(1,t)}{\partial t^2} \quad \text{and } \bar{\gamma}(T_p) = \sqrt{\frac{1}{T_p}\int_0^{T_p} \gamma^2(t)dt} \tag{12}$$

Energy Conservation

Instability leading to droplet formation can be viewed as the conversion of the surface, and fluid film kinetic energy, of the hanging drop at nozzle exit, to the droplets surface energy, droplet kinetic energy in addition to the dissipation due to fluid viscosity being neglected

$$E_{surface} + E_{vib} = \zeta_1 E_{droplets} \tag{13}$$

Expressing $E_{surface} \approx \sigma S_s = \sigma \pi ab$, $E_{vib} \approx \pi M_s f^2 A^2$ and $E_{droplet} = \sum_{i=1}^{N} \sigma S_i = \pi \sigma N \sum_{i=1}^{n} p_i D_i^2$, we deduce

$$\sum_{i=1}^{N} p_i d_i^2 = D_{30} / D_{32} \tag{14}$$

Using the empirical relationship for wave length [10] for ultrasonic spray generator, we take the limit amplitude as $A \approx \zeta_2 (\frac{\mu\sigma}{\rho^2 f^3})^{1/5}$ and then deduce from (13, 14), an analytical expression for the Sauter and Volume Mean Diameter

$$D_{32} = 1/[\rho \frac{\pi}{6\zeta_1}(\frac{ab(\bar{\gamma}+g)}{\sigma\cos\theta_E C} + \frac{f^2}{\sigma}(\zeta_2 \frac{\mu\sigma}{\rho^2 f^3})^{2/5})] \text{ and } D_{30} = \zeta_3 (\frac{\mu\sigma}{\rho^2 f^3})^{1/5} \tag{15}$$

Using Lagrange multipliers we deduce the probability by maximizing the Shannon Entropy $S = -\sum_{i=1}^{n} p_i \ln(p_i)$

Finally the number-based drop-size distribution is deduced using,

$$f_n(D_i) = p_i / \Delta D \tag{16}$$

where we use the fact diameter space is divided into classes noted as [$D_i + \Delta D/2$, $D_i + \Delta D/2$].

ζ_i, i=1,2,3, being constants fixed using our model validation by comparing with experiment.

The previous method is limited by the fact that $f_n(D)$ could lead to non physical results [9,10] where drops of zero sizes seem to exists with a non-zero probability. Whereas the generalized gamma distribution which has been shown to be identical to a Nukiyama-Tanasawa distribution [11], give good results with experiments both for $f_n(D)$ and $f_v(D)$. For our modeling we use the following three-parameter generalized gamma distribution [11]:

$$F_n(D) = \frac{q}{\Gamma(\frac{\alpha}{q})}(\frac{\alpha}{q})^{\frac{\alpha}{q}} \frac{D^{\alpha-1}}{D_{q0}^{\alpha}} \exp[-\frac{\alpha}{q}(\frac{D}{D_{q0}})^q] \tag{17}$$

Our previous physically-based model allows computing two of the three parameters of the generalized gamma distribution. The constraint diameter D_{q0} and parameter α are determined using the following relationship,

$$D_{q0} = \left\{\int_0^{\infty} D^q f_n(D)dD\right\}^{1/q} \quad \text{and} \quad D_{32} = \int_0^{\infty} D^3 F_n(D)dD / \int_0^{\infty} D^2 F_n(D)dD \tag{18}$$

Where $f_n(D)$ is given using (16). The last parameter q is fixed using experimental validation; this parameter is mainly sensitive to atomization process [12]. Thus with this approach, the drop size distribution becomes **dynamic** unlike the classical approach where the parameters have to be adjusted for each operating conditions. The coupling of the previous physical method allow our model to be dynamic and sensitive to physical mechanical and operating conditions of the device.

Experimental Validation

We experimentally determine the drop-size distribution of our new print-head using a new shadow imaging technique [13]. The only adjustment is made in order to find the different constants of the model. Once these parameters determined, the model can predict the other behavior by changing physical and operating conditions taken into account by the model which has a dynamical capability. It is to be noted that the model takes in account the different physical parameters containing in the mean diameters, micro-channel motion, and also the voltage applied to the PZA and the others parameters required for SOD operation.

The following results are prediction of the model with respect to operating conditions and physical properties of the fluid Fig. 2. As an illustration of the model prediction capability is sketched in Fig. 2b three operating vibrating frequency applied to the PZA. Thus an increase in the working frequency favors the production of smaller drops, where an increase of the working frequency decreases the wavelength and therefore reduces the droplet size. These different results are in good agreement with experimental ones [14] for ultrasonic atomizer. In Fig. 2c we have chosen to represent drop-size distribution for 3 different equilibrium contact angle of fluid/structure, such an analysis is out of range for traditional approach of MEF applications. Other capabilities are illustrated in Fig. 2d, where PZA position, a design parameter on nozzle effect is computed.

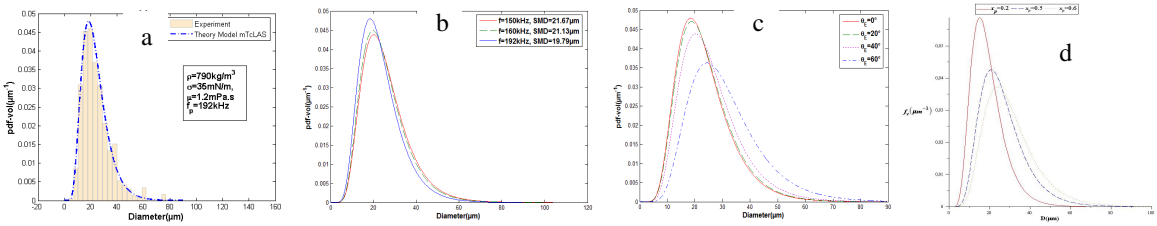

Figure 2. (a) experimental validation; sensitivity to frequency (b) contact angle (c) PZA position effect (d)

Coalescence effect

The characteristics of coalescence occurring between spray droplets, satisfies the following equation [15]

$$\frac{\partial f_n}{\partial t}(V,t) = \frac{1}{2}\int_{V_{min}}^{V} K_c(V-V',V') f_n(V-V') N(t) f_n(V') dV' - f_n(V)\int_{V_{min}}^{V_{max}} K_c(V,V') N(t) f_n(V') dV' \quad (19)$$

Using a Monte Carlo scheme, we compute the number of particles at time t_{n+1} using number particles at time t_n, with $t_{n+1} = t_{n+1} + \Delta t$. Let $X_{N,n}{}^k, 1 \le k \le N$ be N independent real random variables uniformly distributed in $\{1,2...N\}$ and $U_{N,n}{}^k, 1 \le k \le N$ be N independent real random variables uniformly distributed on [0,1]. we assume that all the random variables $X_{N,n}{}^k, 1 \le k \le N$ and $U_{N,n}{}^k, 1 \le k \le N$ are independent. The new sizes of particles $P_N{}^{n+1}(k), 1 \le k \le N$ are defined as:

$$P_N{}^{n+1}(k) = \begin{cases} P_N{}^n(k) + P_N{}^n(X_{N,n}{}^k), & if\ U_{N,n}{}^k < \Delta t K_c(P_N{}^n(k), P_N{}^{n+1}(X_{N,n}{}^k)) \\ P_N{}^n(k) & Otherwise \end{cases} \quad (20)$$

We show that the following scheme is convergent for a symmetric kernel K_c, and allow computing the coalescence effect. We use equation (17) as initial condition $f_n(V, t=0) = F_n(V)$, formulated in terms of volume (V) instead of the diameter (D).

Conclusion

In this paper, we have performed a theoretical formulation of instantaneous drop size distribution and its temporal evolution of a new SOD device. Some results have been validated through experiments. Coupling the results

from the tube motion conveying fluid established thanks to modified Hamilton's principle, a physically based atomization model has been developed for predicting spray droplet size distribution. Maximum Entropy Formalism (MEF) is then used to predict Drop size distribution using experimental measurements for validation purpose. With the use of Sauter Mean Diameter (D_{32}), Volume Mean Diameter (D_{30}), and also the voltage applied to the PZA for fluid/structure motion, we have established a physically based prediction model coupling the three parameter generalized gamma distribution and conservation laws of MEF. The model parameters have been deduced using a limited set of experimental measurements obtained with the SOD. This new dynamic model is capable of predicting drop size distribution for well specified operating conditions, fluid and channel structure properties. This new approach avoids the traditional adjustment for each operating condition and has much better predictive capabilities. Indeed, the model being physically-based is capable of predicting the effect of parameters such as equilibrium contact angle between fluid/channel on the drop size distribution, design parameters like PZA position on nozzle and SOD nozzle length. These dynamics sensitivities of the model make our approach a powerful tool for optimizing the promising SOD device. As a final step, the population balance equation, taking into account the interactions between droplets allows the determination of drop-size distribution evolution. This evolution is shown to be convergent. The device, described in this paper, may be used in a host of innovative microfluidic applications where minute and controlled depositions of highly valued complex fluids are required. Some examples are concern the deposition of metal on substrates or the printing of micro fuel cells.

Nomenclature

a semi-major axis length of nozzle exit shape
b semi-minor axis length of nozzle exit shape
g gravity acceleration (=9.81 $m.s^{-2}$)
L length of the nozzle (=5 10^{-2} m)
N total number of drops
N_i number of drops in each class i
EI channel (or nozzle) flexural rigidity (=1.8398 10^{-2} SI)
ς inner radius of the tube (=0.5 10^{-3} m)
ρ fluid density
μ fluid viscosity
$\bar{\gamma}$ mean acceleration at the nozzle tip
σ fluid surface tension
θ_E equilibrium contact angle fluid/structure

References

1. Yarin, A. L., *Annual Review of Fluid Mechanics*, vol. 38, p. 159-192 (2006).
2. "Liquid Dispensing Apparatus", International Publication Number WO 99/46126, 16, September 1999.
3. Piezoelectric Ceramics: Principles and Applications, by APC International Ltd., ISBN-10: 0971874409, (2002)
4. Housner, G.W., 1952, *Journal of applied Mechanics* vol. 19, p. 205-208 (1952).
5. Païdoussis M.P., Semler, C., Wadham-Gagnon, M., Saaid,S., *Journal of Fluids and Structures*, vol. 23, p. 569-587 (2007).
6. Lin, Y.H, Chu, C.L, *Journal of sound and vibration*, vol. 196, p. 97-105, (1996)
7. I. Prigogine,I., Kondepudi,D., Modern Thermodynamics: From Heat Engines to Dissipative Structures, John Wiley & Sons, 1998.
8. Tembely , M., Lecot, C., and Soucemarianadin,A., *Proceedings of International Conference On Mechanical Engineering, World Congress On Engineering*, pp. 1357-1365, July 2008, London, UK
9. Babinski, E., and Sojka, P. E., *Progress in Energy and Combustion Science*, vol. 28, p. 303–329 (2002)
10. Dobre, M., Caractérisation stochastique des sprays ultrasoniques: le formalisme de l'entropie maximale, Thesis, UCL, 2003.
11. Dumouchel,C. , *Part. Part. Syst. Charact.* vol. 23 pp. 468–479 (2006).
12. Lecompte, M., and Dumouchel,C., *Part. Part. Syst. Charact.,* vol. 25, p. 154 – 167 (2008).
13. Blaisot, J.B. and Yon, J., *Experiments in Fluids*, vol. 39, pp. 977-994 (2005).
14. Dumouchel,C., Sindayihebura,D. and Bolle,L., *Part. Part. Syst. Charact.,* vol. 20, p. 150-161, (2003).
15. Kocamustafaogullari, .G, Ishii, M., *Int J Heat Mass. Transfer* vol. 38 p. 481–493 (1995).